Systems/Circuits

Selective Strengthening of Intracortical Excitatory Input Leads to Receptive Field Refinement during Auditory Cortical Development

Yujiao J. Sun,[1,3] Bao-hua Liu,[1,3] Huizhong W. Tao,[1,2] and Li I. Zhang[1,2]

[1]Zilkha Neurogenetic Institute, [2]Department of Physiology and Neuroscience, and [3]Graduate Program in Physiology and Biophysics, Keck School of Medicine, University of Southern California, Los Angeles, California 90089

In the primary auditory cortex (A1) of rats, refinement of excitatory input to layer (L)4 neurons contributes to the sharpening of their frequency selectivity during postnatal development. L4 neurons receive both feedforward thalamocortical and recurrent intracortical inputs, but how potential developmental changes of each component can account for the sharpening of excitatory input tuning remains unclear. By combining *in vivo* whole-cell recording and pharmacological silencing of cortical spiking in young rats of both sexes, we examined developmental changes at three hierarchical stages: output of auditory thalamic neurons, thalamocortical input and recurrent excitatory input to an A1 L4 neuron. In the thalamus, the tonotopic map matured with an expanded range of frequency representations, while the frequency tuning of output responses was unchanged. On the other hand, the tuning shape of both thalamocortical and intracortical excitatory inputs to a L4 neuron became sharpened. In particular, the intracortical input became better tuned than thalamocortical excitation. Moreover, the weight of intracortical excitation around the optimal frequency was selectively strengthened, resulting in a dominant role of intracortical excitation in defining the total excitatory input tuning. Our modeling work further demonstrates that the frequency-selective strengthening of local recurrent excitatory connections plays a major role in the refinement of excitatory input tuning of L4 neurons.

Key words: **auditory cortex; developmental refinement; synaptic circuit mechanism; thalamocortical projection; tonal receptive field; whole-cell recording**

Significance Statement

During postnatal development, sensory cortex undergoes functional refinement, through which the size of sensory receptive field is reduced. In the rat primary auditory cortex, such refinement in layer (L)4 is mainly attributed to improved selectivity of excitatory input a L4 neuron receives. In this study, we further examined three stages along the hierarchical neural pathway where excitatory input refinement might occur. We found that developmental refinement takes place at both thalamocortical and intracortical circuit levels, but not at the thalamic output level. Together with modeling results, we revealed that the optimal-frequency-selective strengthening of intracortical excitation plays a dominant role in the refinement of excitatory input tuning.

Introduction

Neural circuits in sensory cortices undergo rapid developmental maturation in postnatal stages (Fagiolini et al., 1994; Katz and Shatz, 1996; Zhang et al., 2001; Inan and Crair, 2007), during which cortical functions and organization are extremely susceptible to influences of external environments (Zhang et al., 2001, 2002; Chang and Merzenich, 2003; de Villers-Sidani et al., 2007). In the rat auditory system, after ear canals open at around postnatal day (P)9–P10, cortical responses to acoustic stimuli appear at ~P10–P12 (Romand, 1997; de Villers-Sidani et al., 2007). Within a short period afterward, thalamorecipient layer (L)4 neurons in the primary auditory cortex (A1) gradually acquire adult-like functional properties (Eggermont, 1991; Zhang et al.,

Received Sept. 27, 2018; revised Nov. 17, 2018; accepted Dec. 7, 2018.

Author contributions: Y.J.S. wrote the first draft of the paper; Y.J.S., H.W.T., and L.I.Z. edited the paper; H.W.T. and L.I.Z. designed research; Y.J.S. and B.-h.L. performed research; Y.J.S. analyzed data; H.W.T. wrote the paper.

This work was supported by National Institutes of Health (NIH) Grant R01DC008983 and by the David and Lucile Packard Foundation to L.I.Z., NIH Grants R01EY019049 and R01EY022478 to H.W.T, and NIH Grant K99EY029002 to Y.J.S.

The authors declare no competing financial interests.

Correspondence should be addressed to Li I. Zhang at liizhang@usc.edu or Huizhong W. Tao at htao@usc.edu.

Y. J. Sun's present address: Department of Physiology, University of California San Francisco, San Francisco, CA 94158.

https://doi.org/10.1523/JNEUROSCI.2492-18.2018

 0270-6474/19/391195-11$15.00/0

2001; Chang and Merzenich, 2003), manifested by narrowly tuned spiking receptive fields of individual neurons and a refined tonotopic map across A1 (Zhang et al., 2001; Mrsic-Flogel et al., 2003; Bonham et al., 2004; Kim et al., 2013). This functional refinement is an important determinant for the precise laminar processing, and is achieved primarily through a fine adjustment of excitatory input to individual L4 neurons rather than changing their inhibitory input tuning (Sun et al., 2010; but see Dorrn et al., 2010).

Unlike inhibitory input generated locally in the cortex, the excitatory input to a L4 neuron comes from both thalamocortical and intracortical sources (Read et al., 2002; Winer et al., 2005). In principle, the sharpening of its excitatory input tuning could result from changes at multiple sites along the hierarchical neural pathway (Fig. 1). First, maturation of subcortical nuclei may lead to improved tuning selectivity of neurons in the auditory thalamus, the ventral medial geniculate body (MGBv), resulting in sharpened thalamocortical excitation. Second, modifications of thalamocortical synaptic sites, for example, strengthening of synaptic connections representing optimal frequencies and/or weakening of those representing non-optimal frequencies, can also effectively sharpen the tuning of thalamocortical excitation. Third, recurrent excitatory connections in the cortex may reorganize or modify their synaptic strengths, so that the tuning of intracortical excitation is sharpened. Previous studies have explored some of these potential mechanisms with *in vivo* extracellular or *in vitro* whole-cell recordings (Metherate and Aramakis, 1999; Chang et al., 2005; Barkat et al., 2011). However, because of technical limitations, a definitive conclusion is lacking and direct comparisons of sound-evoked thalamocortical and intracortical excitation to L4 neurons during development have yet to be made.

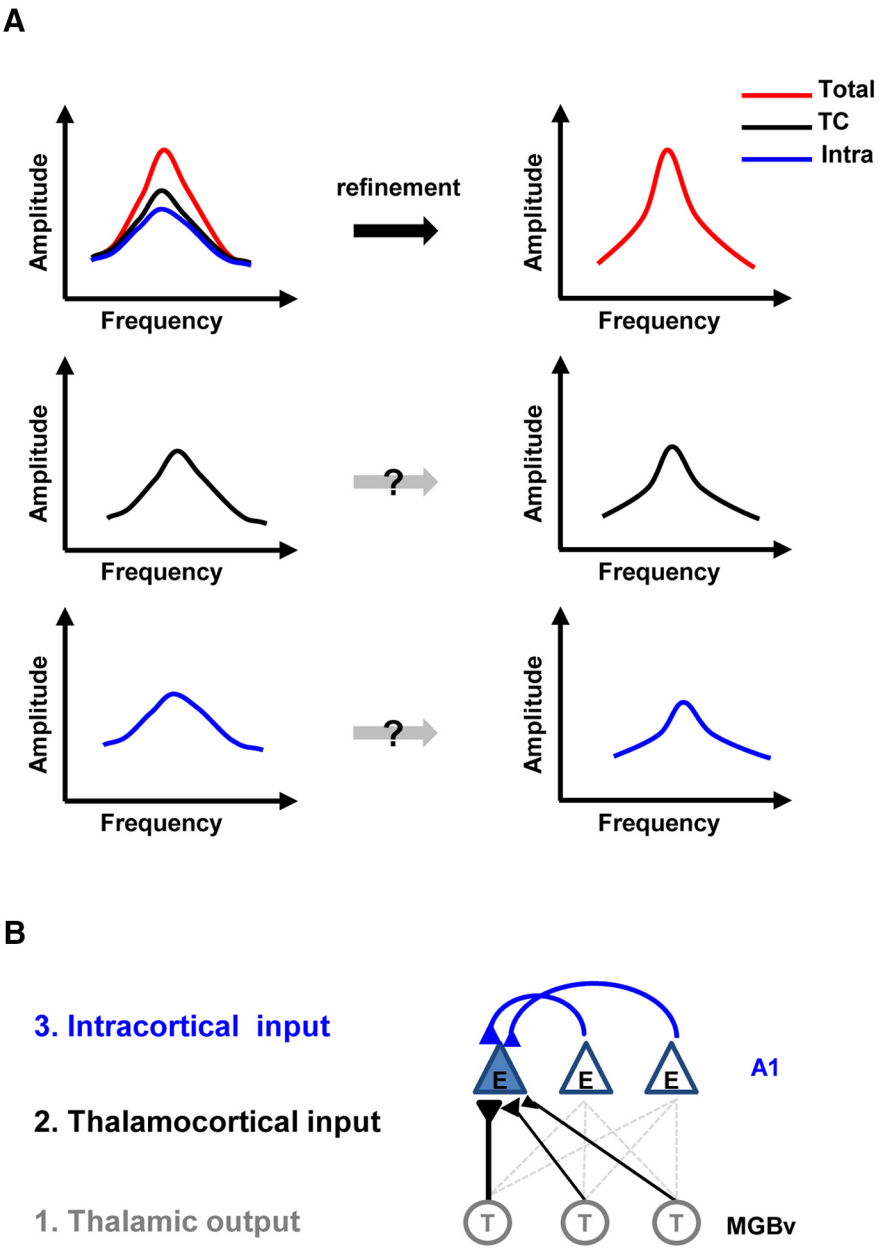

Figure 1. Potential changes during cortical refinement. ***A***, Developmental sharpening of frequency tuning of total excitatory input (red curve, top) to a L4 pyramidal neuron could be contributed by the sharpening of thalamocortical input (black curve, middle), of excitatory intracortical input (blue, bottom), or both. ***B***, Hierarchical structures potentially involved in the refinement: (1) thalamic output response, (2) thalamocortical connections, and (3) intracortical connections from other excitatory neurons in A1.

In this study, by combing *in vivo* electrophysiology and cortical silencing, we examined the circuit mechanisms underlying the improved frequency selectivity of L4 neurons in the rat A1. We did not find significant changes of tuning selectivity of thalamic output responses, except that the range of frequency representations across the thalamic-neuron population was expanded. On the other hand, frequency tuning of thalamocortical and intracortical excitation was sharpened, and intracortical excitation was selectively strengthened at the optimal frequency. Although both contributed to the refinement of total excitatory input, our modeling results suggested that the sharpening and selective strengthening of intracortical excitatory connections play a major role in refining frequency tuning of L4 neurons during development.

Materials and Methods

All experimental procedures used in this study were approved by the Animal Care and Use Committee at the University of Southern California. Sprague-Dawley rats of ages ranging from P15 to P25 and of both sexes were used in this study.

Animal preparation. Experiments were performed in a sound-proof booth (Acoustic Systems) as described previously (Zhang et al., 2001; Tan et al., 2004; Wu et al., 2008). The animals were anesthetized intraperitoneally with ketamine and xylazine (ketamine: 45 mg/kg; xylazine: 6.4 mg/kg). Craniotomy and durotomy were performed to expose the auditory cortex and the ear canal on the same side was plugged. Extracellular recordings were made with a Parylene-coated tungsten electrode (2 MV, FHC) at 500–600 μm depth below the pia. The cortical surface was covered with pre-warmed artificial CSF (in mM: 124 NaCl, 1.2

NaH_2PO_4, 2.5 KCl, 25 $NaHCO_3$, 20 glucose, 2 $CaCl_2$, 1 $MgCl_2$). Frequency-intensity tonal receptive fields of recorded sites were obtained by presenting pure-tone stimuli (0.5–64 kHz at 0.1 octave intervals, 25 ms duration, 3 ms ramp, 0–70 dB sound pressure level at 10 dB increments, a total of 568 testing stimuli) at eight sound intensities, which were delivered through a calibrated free-field speaker to the intact ear. From the tonal receptive fields (TRFs) of spike responses from an array of recording sites, the A1 was located according to the tonotopic gradient, as previously described (Zhang et al., 2001; Wu et al., 2008; Hackett et al., 2011).

Dense mapping of MGBv. Multiunit spikes in MGBv were recorded with a Parylene-coated tungsten electrode (2 MΩ, FHC), which vertically penetrated the brain (2.8~3.6 mm from bregma, 1.7~2.2 mm from midline, 2.8~4.8 mm below the pia surface). MGBv was distinguished from other auditory thalamic regions based on response properties, as previously described (Hackett et al., 2011; L. Y. Li et al., 2013). Signals were amplified (Plexon) and bandpass filtered between 300 and 6000 Hz. TRF was mapped 2–4 times to obtain an average spike receptive field. Characteristic frequency and intensity threshold were determined from the average TRF for each site. Approximately 40–60 individual sites were mapped in each animal to obtain a relatively high-density three-dimensional tonotopic organization. Custom-made software (LabVIEW, National Instruments) was used to extract the spike times. Onset latency was determined as the lag between the stimulus onset and the negative peak of the first evoked spike. Then the overall onset latency of spike responses was chosen as the value at 5% position of the cumulative histogram of all latencies. The firing rate of tone-evoked spikes was counted within a window of 10–50 ms from the onset of tone stimuli.

In vivo *whole-cell voltage-clamp recording and cortical silencing.* After premapping of A1, neurons located at ~450–650 μm depth below the pia, corresponding to the input layer of A1, were specifically targeted for whole-cell recording. After inserting the recording pipette (impedance 4~5 MΩ) into the cortical tissue, we applied agar (3.5%) to minimize cortical pulsation. For voltage-clamp recording, the pipette solution contained the following (in mM): 125 Cs-gluconate, 5 TEA-Cl, 4 MgATP, 0.3 GTP, 10 phosphocreatine, 10 HEPES, 1 EGTA, 2 CsCl, 1.5 QX-314, 1% biocytin or 2.5 fluorescein dextran, pH 7.2. As we previously reported and discussed (Liu et al., 2007; Wu et al., 2008), the recording condition (with a relatively large pipette tip size) resulted in sampling of almost exclusively pyramidal neurons. Recordings were made with an AxoPatch 200B amplifier (Molecular Devices). The whole-cell and pipette capacitance (30–70 pF) were completely compensated and the initial series resistance (20–50 MΩ) was compensated for 50% to achieve an effective series resistance of 10–25 MΩ. Signals were filtered at 5 kHz and sampled at 10 kHz. Only neurons with resting membrane potentials more hyperpolarized than −55 mV were used for further analysis. To obtain tone-evoked excitatory synaptic responses, neurons were clamped at −70 mV, which was around the reversal potential for inhibitory currents. Synaptic TRFs were mapped for 3 trials.

The cortex was pharmacologically silenced either before or during the whole-cell recording following the method established in our previous studies (Liu et al., 2007; Zhou et al., 2010; Sun et al., 2013). A mixture of SCH50911 (6 mM; a specific antagonist of $GABA_B$ receptors) and muscimol (4 mM; an agonist of $GABA_A$ receptor) was applied to effectively silence a local cortical region without affecting thalamic areas. A glass micropipette with a tip opening of 2–3 μm in diameter was inserted to a depth of 450–500 μm beneath the cortical surface. Solutions (cocktails dissolved in ACSF containing Fast Green) were slowly injected under a pressure of 2–3 psi for 5 min. The staining by Fast Green, as monitored under the surgical microscope, covered a cortical area within a radius of ~1 mm by the end of the injection. The successful application of the drug was further confirmed by the absence of inhibitory currents when the cell was clamped at 0 mV (data not shown). The injected volume was ~10–50 nl, as measured in mineral oil. The stable recording quality before and after the injection was judged by <20% change of series resistance during the course of the experiment as well as unchanged response onset latencies and CF (see Fig. 3*B*,*C*), consistent with our previous observations (Liu et al., 2007; Zhou et al., 2010; L. Y. Li et al., 2013; Sun et al., 2013).

Data analysis. Tone-evoked synaptic responses were identified according to their onset latencies and peak amplitudes. The onset latency was identified during the rising phase of the response trace as the time point where the current amplitude exceeded 2 SD of baseline fluctuations. Only responses with latencies within 10–50 ms from the onset of tone stimulus, and with peak amplitude larger than three SDs of baseline fluctuations, were considered as evoked responses.

Tuning curves were reconstructed according to the pseudorandom sequence of tonal presentations. Characteristic frequency (CF) was defined as the frequency that evoked a reliable response at the lowest intensity level, the intensity threshold. Tuning bandwidths were determined at 20 dB above the intensity threshold. First, the total frequency responding range at 20 dB above threshold (i.e., BW20) was determined based on the continuity of significantly evoked responses in the frequency domain. Second, to quantify the shape of the synaptic tuning curve, an envelope curve was derived based on the peak amplitude of each synaptic response within the total frequency responding range by using MATLAB software Envelope 1.1 (MathWorks), which identifies the local maxima and minima in the raw dataset and generates a smooth envelope with cubic Hermite interpolation. The full-width at half-maximum (FWHM) was then defined as the frequency range for responses >50% of the maximum.

Modeling. We built a two-layer neural network consisting of a first layer of feedforward excitatory neurons and a second layer of interconnected excitatory and inhibitory cells. The first layer corresponds to a population of auditory thalamic neurons, with their characteristic frequencies systematically varied and each exhibiting a skewed Gaussian tuning curve for the output response (Liu et al., 2010). The output ψ of a thalamic unit T_c in response to a pure tone stimulus f is described as follows:

$$\psi_{T_c}(f) = e^{-\frac{(f-c)^2}{2\omega^2}} \int_{-\infty}^{\alpha_c \frac{f-c}{\omega}} e^{-\frac{t^2}{2}}\, dt. \quad (1)$$

Where c is the characteristic frequency of the unit, f is the sound frequency of the stimulus, ω represents the tuning bandwidth of the unit (assumed to be the same for all units, as the bandwidth is not significantly different for neurons with different characteristic frequencies), and a_c shows the degree of the skewedness, varying from −1 to 1 for units with low-to-high characteristic frequency to represent their asymmetric tuning shape.

Theses thalamic units are connected to the cortical layer by a center-weighted Gaussian connectivity function W_{TC}:

$$W_{T_jC_i} = e^{-\frac{(c_j-c_i)^2}{2\sigma^2}}. \quad (2)$$

Where c_j is the characteristic frequency of the thalamic unit T_j and c_i is the characteristic frequency of the cortical unit C_i (either excitatory or inhibitory). The variable σ determines the sharpness of the thalamocortical connectivity and changes through refinement.

The cortical layer consists of excitatory and inhibitory units with a number ratio of 4:1. They are simple linear integrators with thresholding nonlinearity (i.e., its firing rate is proportional to its input, except that subthreshold inputs produce a zero firing rate). The output of each cortical unit ψ_c ($C \in E, I$) is thus calculated by thresholding its total input x (Seybold et al., 2015):

$$\psi_C(x) = \gamma_c \cdot max(x - \Gamma_c, 0). \quad (3)$$

Where Γ_c is the threshold of the unit and γ_c is the coefficient for input-output transformation. The two parameters are separately set for excitatory and inhibitory units so that inhibitory units are more responsive than excitatory units. And the synaptic inputs x_{Ci} ($c \in E, I$) are calculated as follows:

$$x_{C_i} = \sum_{j \in T} W_{T_jC_i}\psi_{T_j} + \sum_{j \in T} W_{E_jC_i}\psi_{E_j} - \sum_{j \in I} W_{I_jC_i}\psi_{I_j}. \quad (4)$$

Where ψ_T, ψ_E, and ψ_I are outputs of thalamic, cortical excitatory and inhibitory units, respectively, whereas W_{TC}, W_{EC}, and W_{IC} are the corresponding connectivity weights onto the cortical unit C_i. Similar to thalamocortical connectivity, the inhibitory connectivity W_{IC} also has a Gaussian connectivity function with the connectivity shape remaining the same throughout development, based on reported experimental results (Sun et al., 2010). The excitatory connectivity W_{EC} follows an exponential distribution:

$$W_{E_jC_i} = \Theta \cdot e^{\lambda|c_j - c_i|}. \quad (5)$$

Where c_j and c_i are the characteristic frequencies of two cortical units. Two variables λ and Θ define the sharpness and strength (relative to that of thalamocortical connectivity), respectively.

We set the initial parameters to match the experimental data before the refinement, by varying the three free parameters (Antolík et al., 2016): sharpness of thalamocortical connectivity σ, sharpness of intracortical connectivity λ and its strength relative to thalamocortical connectivity Θ.

Statistical methods. Results were plotted as conventional box-and-whisker plots with whiskers denoting SD. Unpaired Student's *t* test was performed for the comparisons between different age groups, because data fit into normal distributions. For Figure 4, *A* and *B*, results were tested by the Wilcoxon matched-pairs test (the nonparametric version of one-sample *t* test) and fitted using linear regression with the coefficient of determination (R^2) reported. For Figure 4*C–F*, one-way ANOVA tests were used to test multiple matched samples and *post hoc* Scheffe test was applied to compare the means for all possible combinations of two data groups.

Results

Major functional refinement of neurons in the rat A1 occurs during the third postnatal week (Zhang et al., 2001, 2002; Chang et al., 2005), during which the frequency tuning of excitatory input to individual L4 neurons sharpens (Sun et al., 2010). In this study, we focused on animals aged P15–P17 and P20–P25, two developmental stages before and after the functional refinement, respectively (Sun et al., 2010).

Frequency tuning of thalamic output responses is unchanged during the functional refinement

We first characterized subcortical output responses to auditory stimuli by recording from MGBv neurons in animals of the two different age groups (see Materials and Methods). We obtained a three-dimensional tonotopic map (Fig. 2*A*,*B*, left) from recordings of 40–60 microelectrode penetration sites in each animal. For each recording site, we reconstructed a frequency-intensity TRF (Fig. 2*A*,*B*, right) from multiunit spiking responses to brief tone pips of varying frequencies and intensities and determined the CF, the frequency at which tones could evoke significant responses at the lowest intensity. Consistent with previous reports (Romand, 1997; Barkat et al., 2011), a low-to-high CF gradient was observed along the dorsolateral-to-ventromedial axis in MGBv (Fig. 2*A*,*B*, left). Before the functional refinement, thalamic responses exhibited CFs within a low- to mid-frequency range (4–24 kHz), whereas after the refinement the CFs expanded to a broader range such that representations of lower and higher frequencies appeared (Fig. 2*C*), reminiscent of several previous studies (Zhang et al., 2001; de Villers-Sidani et al., 2007; Polley et al., 2013). To quantify the developmental progression for thalamic responses, we measured the total frequency responding range at 20 dB above the intensity threshold (i.e., BW20), which reflects the extent of frequency tuning at this intensity (see Materials and Methods). We found no significant differences in BW20 between the two developmental stages within each CF range although the total CF range expanded (Fig. 2*C*). We also compared other response features before and after the refinement. Overall, the mean response onset latency became shorter (Fig. 2*G*, black), indicating faster responses in the more matured auditory thalamus. The average evoked firing rate slightly increased developmentally (Fig. 2*H*, black). The intensity threshold of TRF exhibited a trend of developmental decrease, but this change has not reached statistical significance (Fig. 2*I*, black). Together, our results indicate that the changes at the thalamic output level cannot account for the sharpening of excitatory input to thalamorecipient L4 neurons. Instead, changes occurring within the cortex are more likely to play a role in the developmental refinement.

Thalamocortical input tuning is sharpened during the functional refinement

We next measured the thalamocortical input to L4 neurons. Following our previously established procedures (Liu et al., 2007), we silenced cortical spiking activity by injecting a mixture of muscimol and SCH90511 at ~500 μm depth below the pia, which effectively eliminates cortical spikes within a radius of 500 μm of the injection site without affecting auditory thalamic responses or presynaptic release at thalamocortical synapses (Liu et al., 2007; Sun et al., 2013). In the animals with cortical spikes silenced, we then performed *in vivo* whole-cell voltage-clamp recordings from L4 neurons and recorded their excitatory synaptic responses to tones by clamping the cell's membrane potential at −70 mV, the reversal potential of inhibitory currents (see Materials and Methods). Because cortical spikes were blocked, intracortical inputs were abolished and the recorded evoked excitatory response was reflective of the isolated thalamocortical input to L4 neurons (Liu et al., 2007). By comparing TRFs of thalamocortical input in neurons of different age groups, we found that the tuning shape of thalamocortical input became sharper after the refinement (Fig. 2*D*,*E*, envelope curve within the red box). For the quantification of synaptic input tuning, we measured the total frequency responding range at 20 dB above the intensity threshold (BW20) as well as the FWHM which reflects the strength of tuning. The BW20 was not significantly different before and after the refinement (Fig. 2*F*, white), but the FWHM became significantly reduced after the refinement (Fig. 2*F*, gray). These results indicate that while the overall thalamocortical connections to a L4 neuron remain stable over the period of development, their strengths are finely adjusted so that the tuning selectivity is improved. As for other response parameters, the onset latency of thalamocortical excitation became significantly shortened after the refinement (Fig. 2*G*, gray), consistent with the observation of faster spiking responses of thalamic neurons (Fig. 2*G*, black). The speeding up of thalamocortical input could also be contributed by a progressive myelination of thalamocortical axons during early development (Romand, 1997; Salami et al., 2003; Etxeberria et al., 2016). The amplitude of thalamocortical excitation, as measured by the peak amplitude of the maximal response within the receptive field, was not significantly changed over the period of development (Fig. 2*H*, gray), despite the increased thalamic firing rate (Fig. 2*H*, black). This suggests a possible overall reduction of thalamocortical synaptic strength at the postsynaptic site. The intensity threshold of TRF of thalamocortical excitation remained unchanged (Fig. 2*I*, gray), consistent with the unchanged intensity threshold of thalamic spiking responses (Fig. 2*I*, black). We also measured the input resistance of the L4 neurons and found no significant difference between the two age groups (333.3 ± 72.3 MΩ before vs 352.2 ± 65.2 MΩ after, mean ± SD, $n = 19$ and 20 cells, respectively; $p = 0.63$, *t* test), consistent with the results of previous developmental studies on auditory cortical

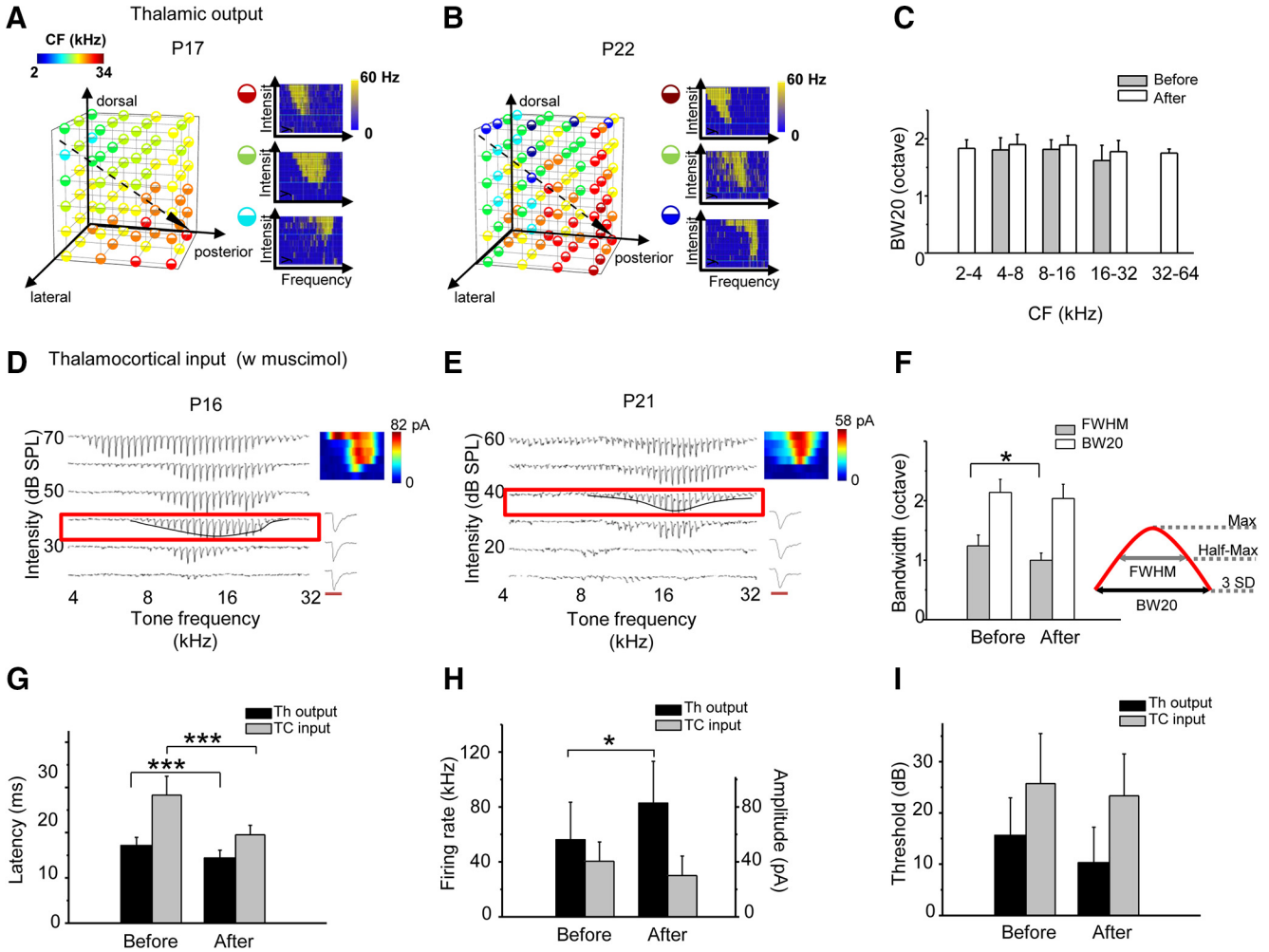

Figure 2. Thalamic output responses during cortical development and a refinement of thalamocortical input. ***A***, ***B***, Left, The 3-D tonotopic map in MGBv of an example P17 and a P22 animal. Each dot represents one recording site, with color indicating its CF. Dashed arrow indicates the axis for the low-to-high CF gradient. Right, Color maps show the TRFs of three example sites with low, mid, and high CFs, respectively, with *x*-axis representing the tone frequency and *y*-axis representing the tone intensity. Brightness of yellow color indicates the level of evoked firing rates. ***C***, Average BW20 of MGBv responses within each CF range in animals of two different stages. $N = 3, 3$ animals; $n = 17, 25, 10$ sites for three CF ranges before refinement and $n = 5, 15, 15, 23, 8$ sites for five CF ranges after refinement. No significant difference, ANOVA test. All bars represent SD. ***D***, ***E***, TRFs of excitatory input for an example P16 and a P21 neuron. Each small trace represents the average excitatory synaptic current (from 3 trials) evoked by a pure tone of a specific frequency and intensity. Black envelope curve within the red box outlines the frequency tuning curve at 20 dB above the intensity threshold. Color map in the top right corner depicts the peak amplitude of each evoked response in the frequency-intensity space, and below the color map are responses evoked by the CF tone (50 ms, duration marked by the red line) in three individual trials. ***F***, Average BW20 (white) and FWHM (gray) of thalamocortical excitation before and after the refinement ($n = 12$ and 14 cells respectively). $^*p < 0.05$, *t* test. Inset, Illustration of how BW20 and FWHM are measured from the frequency tuning curve. ***G***, Average onset latency of thalamocortical excitation (gray, $n = 12$ and 14) and thalamic spiking responses (black, $n = 52$ and 66) evoked by CF tones before and after the refinement. $^{***}p < 0.001$, *t* test. Th, thalamic; TC, thalamocortical. ***H***, Average peak amplitude of thalamocortical excitation (gray, $n = 12$ and 14) and average firing rate of thalamic spiking responses (black, $n = 52$ and 66) evoked by CF tones. $^*p < 0.05$, *t* test. ***I***, Average intensity threshold of TRF of thalamocortical excitation (gray, $n = 12$ and 14) and of thalamic spiking responses (black, $n = 52$ and 66). All bars represent SD.

neurons (Metherate and Aramakis, 1999; Liang et al., 2018). Together, our results demonstrate that the tuning of thalamocortical excitation sharpens during the developmental refinement, likely due to a fine-scale adjustment of strengths of thalamocortical connections.

Intracortical excitation is selectively strengthened and sharpened

To study the developmental change of intracortical excitatory input, we recorded tone-evoked excitatory responses before and after cortical silencing in the same L4 neurons in another cohort of animals at the corresponding ages (Fig. 3*A*,*B*, top and middle). We then derived the intracortical excitation by subtracting the thalamocortical excitation recorded after cortical silencing from the total excitation recorded before cortical silencing (Fig. 3*A*,*B*, bottom). We first confirmed that the onset latency of thalamocortical input and the CF of thalamocortical TRF were comparable to those of the total excitation (Fig. 4*A*,*B*). Such results support the notion that thalamocortical input primarily defines important tuning features of excitation in thalamorecipient neurons (Liu et al., 2007; L. Y. Li et al., 2013). The BW20 of each excitatory input component remained unchanged over the period of development (Fig. 4*C*), further supporting the conclusion that thalamocortical inputs have largely defined the extent of frequency tuning of synaptic inputs throughout development.

Notably, the tuning shape (as reflected by FWHM) of each excitatory input component became sharpened, but to a different degree (Fig. 4*D*). Before the refinement, intracortical excitation was very broadly tuned, so that the tuning of total excitatory input was broader than that of thalamocortical excitation. In other words, intracortical excitation has deteriorated the tuning selectivity. However, after the refinement, the tuning of intracor-

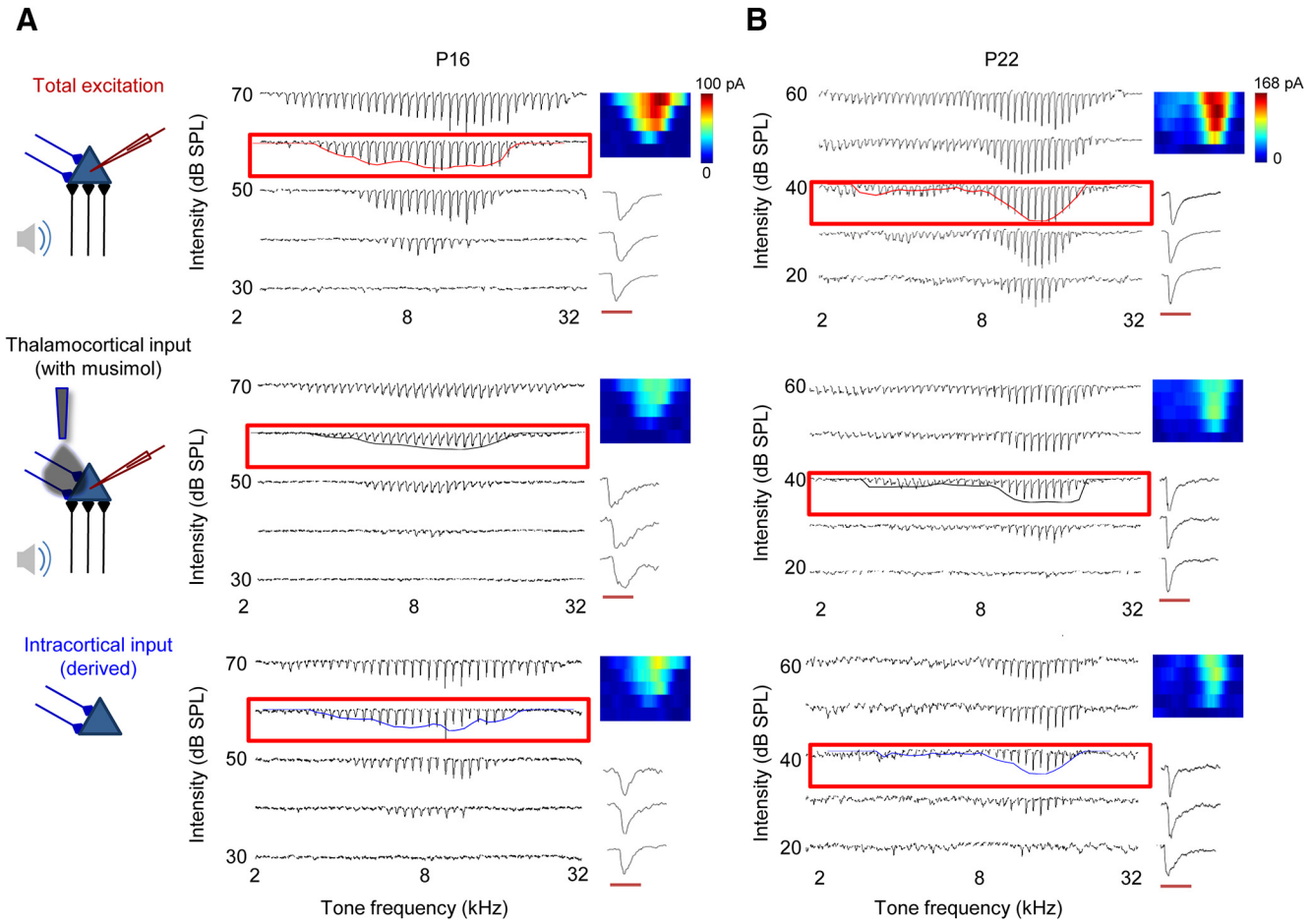

Figure 3. Dissecting different components of excitatory input to a L4 neuron. ***A***, Left, Illustration of the strategy to obtain different components of excitatory input. Middle, TRFs of excitatory responses of an example P16 neuron in the normal condition (top), after cortical silencing (middle), and after subtracting thalamocortical excitation from the total excitation (bottom). Tuning curves at 20 dB above the intensity threshold are outlined with red (total excitation), black (thalamocortical), and blue (intracortical) curves, respectively, within the red box. Right, Color map for synaptic amplitudes in the frequency-intensity space (top) and responses evoked by the CF tone in three trials (bottom). ***B***, Recording from an example P22 neuron. Data are displayed in a similar manner as in ***A***.

tical excitation became greatly sharpened (to a degree larger than that of thalamocortical input), so that the total excitation became better tuned than the thalamocortical excitation (Fig. 4*D*). To further quantitatively understand the relative contributions of different components to the sharpening of excitatory input tuning, we calculated the response amplitude ratio of thalamocortical versus total excitation (Fig. 4*E*). Before the refinement, thalamocortical excitation accounted for over half of the total excitation at both the optimal frequency (CF) and non-optimal frequencies at the edges (edge) of the synaptic receptive field. After the refinement, the contribution of thalamocortical excitation markedly dropped at the CF, indicating a greater contribution of intracortical excitation which increased from 42.1 ± 6.5% to 74.7 ± 2.5%. On the other hand, the contribution of thalamocortical excitation remained largely unchanged at non-optimal frequencies (Fig. 4*E*), indicating a non-equal contribution of intracortical excitation across different frequencies at later stages. Furthermore, a direct comparison of intracortical excitation and thalamocortical excitation demonstrated that their frequency ranges were always similar over the period of development (Fig. 4*F*, BW20). However, after the refinement intracortical excitation became more sharply tuned than thalamocortical excitation (Fig. 4*F*, FWHM) and its contribution to response amplitude at the CF became much greater than thalamocortical excitation (Fig. 4*F*, Amp_CF). Together, our data suggest that the initially broadly tuned intracortical excitatory input becomes selectively strengthened at the optimal frequency, leading to markedly improved frequency tuning of total excitatory input.

Sharpening and selective strengthening of intracortical connectivity plays a major role

As we have observed changes of both thalamocortical and intracortical excitatory inputs, we then ask how these circuit components interact to contribute to the refinement of total excitatory input. To answer this question, we applied circuit modeling to dissociate the changes of thalamocortical versus intracortical connectivity. Our model contained a layer of feedforward thalamic neurons and a layer of interconnected L4 neurons including both excitatory and inhibitory cells (see Methods and Materials). The initial parameters for connectivity settings and synaptic strengths were chosen to match the experimental observations before the refinement, i.e., thalamocortical excitation was better tuned than intracortical excitation and the relative contribution of thalamocortical excitation was similar at the optimal and non-optimal frequencies (compare Figs. 5*A*, 4*D*,*E*). We then systematically studied how circuit reorganizations at thalamocortical and intracortical levels might affect the tuning shape of total excitatory input (as measured by FWHM) by varying selec-

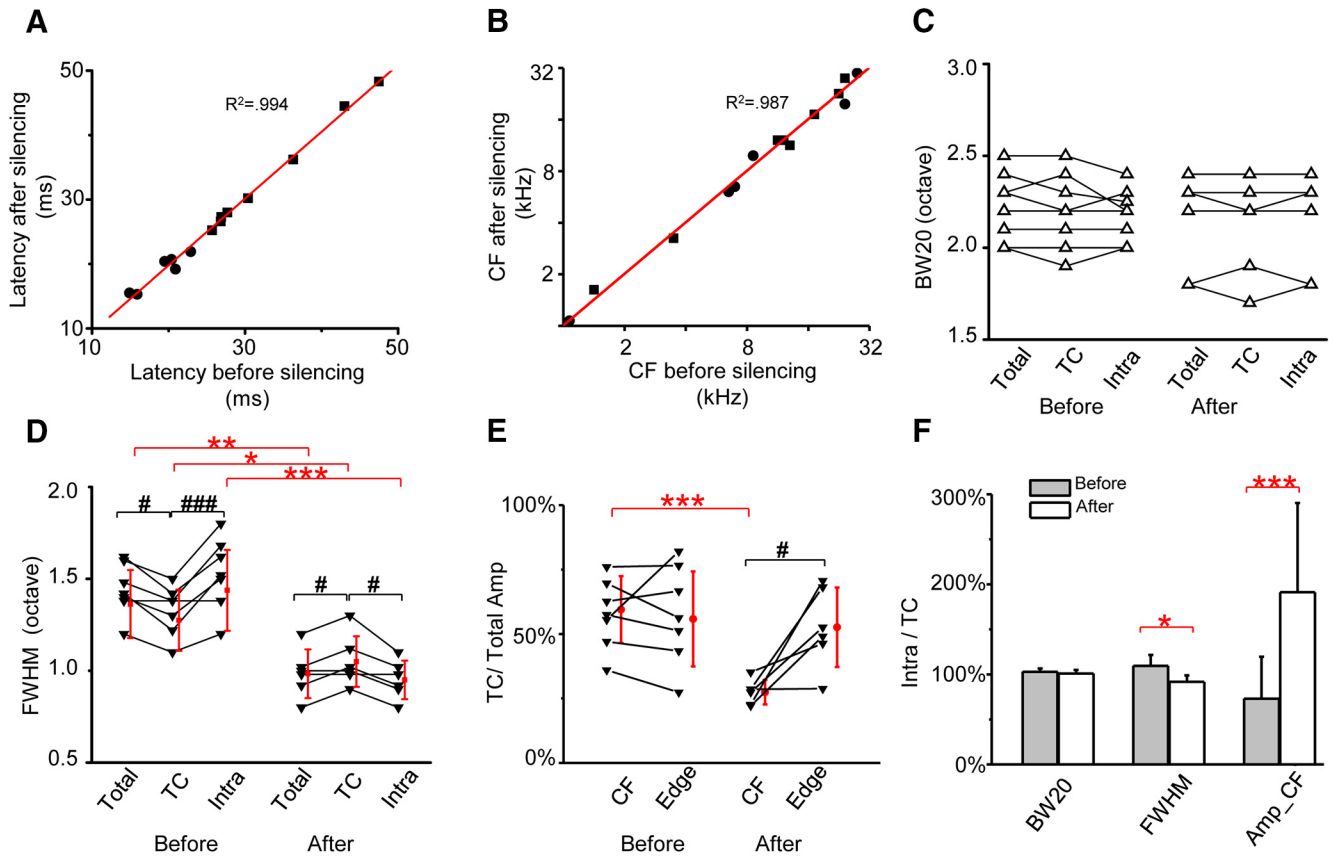

Figure 4. Sharpening and selective strengthening of intracortical excitation during development. ***A***, Onset latencies of CF-evoked excitatory responses after versus before cortical silencing. Each symbol represents one cell. Red line is the unity line. ***B***, CFs of synaptic TRFs after versus before cortical silencing. ***C***, BW20 of total, thalamocortical, and intracortical excitatory input before and after the refinement. Data points for the same cell are connected with lines. $n = 7$ and 6 cells. No significant difference, one-way ANOVA. ***D***, FWHM for the tuning of total, thalamocortical, and intracortical excitation before and after the refinement. Red symbol represents mean ± SD. $n = 7$ and 6 cells. $^{*}p < 0.05$, $^{**}p < 0.01$, $^{***}p < 0.001$, *t* test. $^{\#}p < 0.05$, $^{\#\#\#}p < 0.001$, one-way repeated ANOVA. ***E***, Ratio of peak amplitude of thalamocortical versus total excitation at the CF and receptive field edges before and after the refinement. $n = 7$ and 6. $^{***}p < 0.001$, *t* test. $^{\#}p < 0.05$, paired *t* test. ***F***, Intracortical/thalamocortical ratios for three measures (BW20, FWHM, peak response amplitude evoked by a CF tone) before and after the refinement. $^{*}p < 0.05$, $^{***}p < 0.001$, *t* test.

tivity of thalamocortical and intracortical connectivity independently (Fig. 5*B*). To better illustrate the results, we presented FWHM of thalamocortical, intracortical and total excitation when varying one set of connectivity while keeping the other set fixed (Fig. 5*C*,*D*, slices of Fig. 5*B*). We first examined how thalamocortical connectivity might affect the tuning shape with fixed intracortical connectivity (Fig. 5*C*). When intracortical connectivity was relatively unselective, as in the before-refinement condition, sharpening of thalamocortical connectivity alone resulted in refined tuning of total excitatory input, but without affecting much the tuning of intracortical excitation (Fig. 5*C*, left). As a result, intracortical excitation was always more broadly tuned than thalamocortical excitation, which is inconsistent with our experimental observation. In addition, it becomes less and less effective for thalamocortical connectivity to drive the sharpening of total excitatory input, as manifested by the increased distance between FWHMs of total excitatory input and thalamocortical excitation (Fig. 5*C*, left, compare red and black plots). We next adjusted the intracortical connectivity to a more selective state (Fig. 5*C*, right). This increased selectivity of intracortical connectivity did not affect the tuning of thalamocortical excitation (Fig. 5*C*, left and right, compare black plots), because the latter is purely feedforward. Notably, under the condition of more refined intracortical connectivity, intracortical excitation became more sharply tuned than thalamocortical excitation (Fig. 5*C*, right, compare blue and black plots) and was sensitive to the change of thalamocortical connectivity, making the latter more effective in driving the refinement of total excitatory input (Fig. 5*C*, left and right, compare slopes of the red plots).

We next examined the effect of varying intracortical connectivity alone, which did not affect the tuning of thalamocortical excitation (Fig. 5*D*, black plot). Tuning of total excitatory input became sharpened with increasing intracortical selectivity in both conditions of low and high levels of thalamocortical selectivity, but the effect eventually saturated (Fig. 5*D*, left and right, red plots). Comparing the two different conditions, improved thalamocortical selectivity appeared to have a "subtractive" effect by shifting down FWHMs of intracortical and total excitation (Fig. 5*D*, compare left and right). In other words, thalamocortical connectivity might set a limit for the maximum selectivity that could possibly be achieved. Notably, when intracortical excitation became better tuned than thalamocortical excitation (Fig. 5*D*, intersection of blue and black plots), the tuning selectivity of total excitatory input closely followed that of intracortical excitation. In other words, the component with more refined tuning contributes more importantly to the tuning selectivity of total excitatory input.

We also examined the effects of varying thalamocortical and intracortical selectivity on the relative response amplitude (i.e., amplitude ratio of thalamocortical vs total excitation; Fig. 5*E*). No matter how the connectivity selectivity was manipulated, the amplitude ratio at the optimal frequency (CF) remained constant

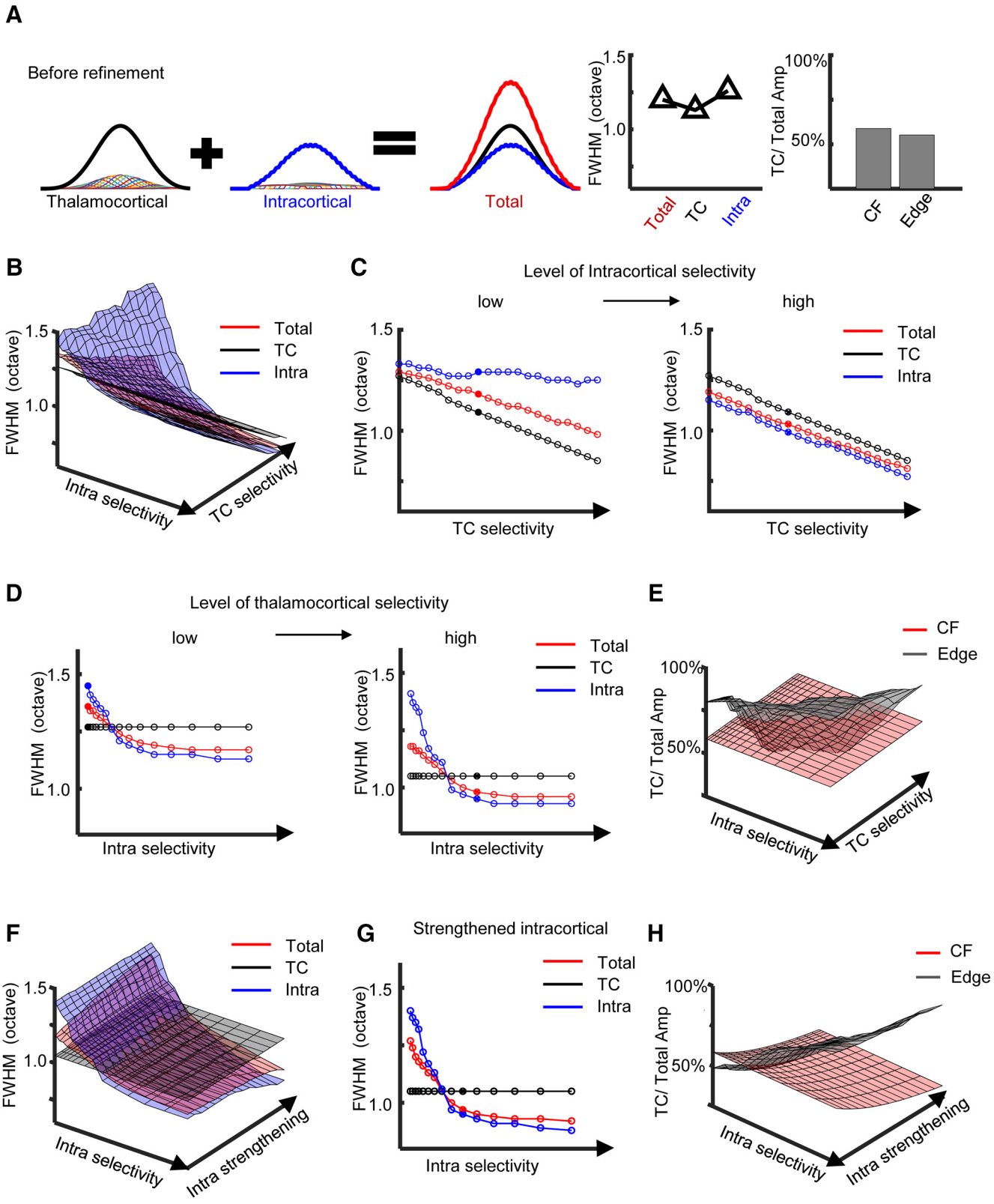

Figure 5. Sharpening and strengthening of intracortical connectivity plays a major role in the refinement. ***A***, Initial parameters of the model were chosen to match the before-refinement experimental observations, including tuning properties of thalamocortical (black envelope) and intracortical (blue envelope) excitation (left and middle) and amplitude ratios of thalamocortical versus total excitation at CF and receptive field edges (right). Thin colored traces represent example tuning curves of individual thalamocortical or intracortical inputs. ***B***, Two variables in the model, selectivity of thalamocortical and intracortical connections, were systematically varied to investigate the effects on the tuning shape (as reflected by FWHM) of each excitatory component. Increasing selectivity of either one could drive a sharpening of the tuning of total excitatory input. ***C***, FWHM for the tuning of thalamocortical (black), intracortical (blue) and total (red) excitation along with increasing selectivity of thalamocortical connectivity, in the conditions of low- (as in before-refinement; left) and high-level (right) intracortical selectivity. ***D***, FWHM for the tuning of thalamocortical (black), intracortical (blue), and total (red) excitation along with increasing selectivity of intracortical connectivity, in the conditions of low- (as in before-refinement; left) and high-level (right) thalamocortical selectivity. ***E***, Amplitude ratio of thalamocortical versus total excitation at the CF (pink) or receptive field edges (gray) with increasing selectivity of (*Figure legend continues.*)

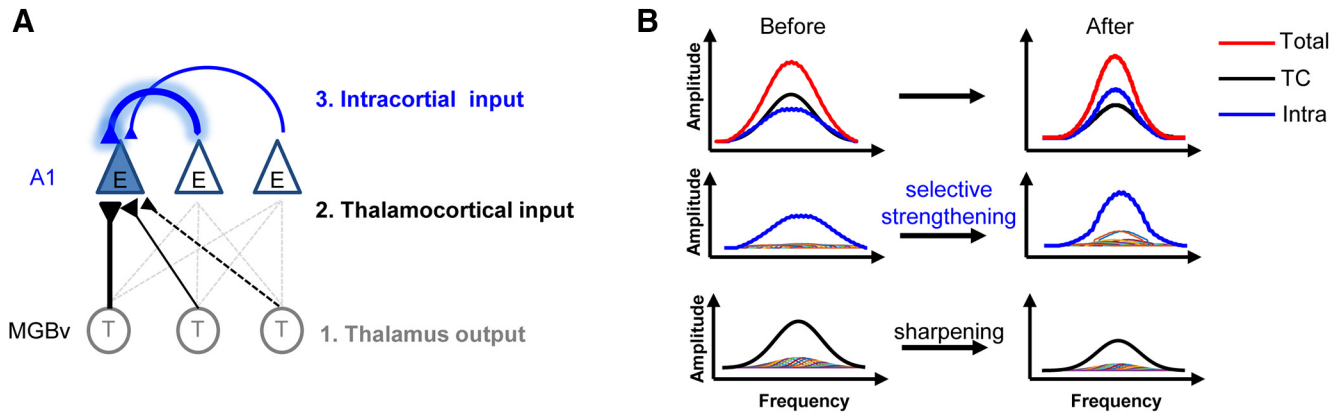

Figure 6. A working model. ***A***, Schematic illustration of circuitry mechanisms underlying sharpened excitatory input tuning in L4 neurons based on our experimental data and modeling results: (1) unchanged output responses from the thalamus (gray circles), (2) refined thalamocortical excitation by adjusting the weights of individual thalamocortical inputs (black projecting lines), (3) selective strengthening of intracortical inputs from similarly tuned (nearby) A1 neurons (blue projecting curves). ***B***, Tuning curve changes before and after the refinement. Note that these tuning curves are relative, normalized to the peak of tuning of the total excitation at the corresponding age.

(Fig. 5*E*, pink). This is inconsistent with our experimental observation, suggesting that additional amplitude adjustments are needed. On the other hand, the amplitude ratio at non-optimal frequencies (edge) increased with greater intracortical selectivity or reduced with greater thalamocortical selectivity (Fig. 5*E*, gray).

Finally, we tested additional amplitude adjustments by scaling up the strengths of intracortical connections (Fig. 5*F*). With the same thalamocortical selectivity, this did not change the trend of bandwidth changes qualitatively but slightly further enhanced the tuning selectivity of total excitatory input (Fig. 5, compare *G*, *D*, right). However, this synaptic strengthening appeared to be the only factor leading to a change of relative response amplitude consistent with our experimental observation, i.e., decreased relative contribution of thalamocortical excitation at the CF with increasing intracortical selectivity (Fig. 5*H*, pink). Together, our results demonstrate that while changes of both thalamocortical and intracortical connectivity can contribute to the sharpening of excitatory input tuning, the increased selectivity and strength of intracortical excitation plays a more dominant role.

Discussion

In this study, we intend to dissect circuit mechanisms for the refinement of excitatory input tuning in L4 pyramidal neurons during development of rat A1. Using a well-established pharmacological method of silencing cortical spiking, we have been able to isolate the thalamocortical and intracortical components of excitatory input to individual L4 neurons. The results are summarized by Figure 6. Although there are no significant changes in the frequency tuning of thalamic spiking responses, the tunings of thalamocortical and intracortical excitatory inputs both became more selective. Initially, thalamocortical input is better tuned than intracortical excitatory input and accounts for ~60% of the total excitation. After refinement, its tuning is slightly sharpened, and its weight contribution drops to <30% at the optimal frequency. In comparison, the initially broadly tuned intracortical excitatory input undergoes a more pronounced sharpening process and becomes a much more dominant contributor to the total excitation, indicating increasing functional importance of local cortical circuits in sensory processing over development. Our modeling results further demonstrate that the reorganization of intracortical connections resulting in frequency-selective strengthening of intracortical excitation plays a major role in the refinement of excitatory input tuning.

Maturation of subcortical pathways

In the first-order auditory thalamus that provides input to A1, we show that the tonotopic map is initially incomplete in that frequency representations are restricted within a low- to mid-frequency range. Representations of lower and higher frequencies appear at later stages. It is worth noting that this result does not imply that neurons do not respond to high-frequency tones at all at earlier stages, but that neurons specifically tuned to high frequencies are lacking, consistent with previous observations in the developing auditory cortex of rats at corresponding ages (Zhang et al., 2001; de Villers-Sidani et al., 2007; Polley et al., 2013). The observed change of the range of tonotopic representation is also consistent with previous results that behavioral responses are first elicited by relatively low-frequency sound stimuli during development (Ehret, 1983).

Refinement of thalamocortical input

Our recordings of multiunit spike activity show that the frequency tuning of thalamic spiking responses is not significantly changed over the period of development. It is worth noting that the multiunit recording does not resolve tuning properties of individual thalamic neurons but more likely assays synchronous firing of multiple thalamic neurons. Nevertheless, combining with the result that the total frequency responding range (BW20) of thalamocortical input is preserved (Fig. 2*F*), the most parsimonious explanation is that the tuning of thalamic neurons is unchanged and that the thalamocortical connectivity has been established earlier than the stages examined and remains relatively stable, i.e., without pruning of existing thalamocortical connections. The sharpened tuning of thalamocortical input after refinement might reflect selective strengthening/weakening of presynaptic release from thalamocortical axons (Blundon et al., 2011; Chun et al., 2013), preferential subcellular positioning of some thalamocortical synapses at more perisomatic sites on L4

←

(*Figure legend continued.*) intracortical or thalamocortical connectivity. ***F***, FWHM for the tuning of different components with increasing intracortical selectivity and strength of intracortical connectivity, in the condition of high-level thalamocortical selectivity (as in ***D***, right). ***G***, One slice of ***F*** representing a situation after scaling up intracortical connectivity strength. ***H***, Amplitude ratio of thalamocortical versus total excitation with increasing intracortical selectivity and strength of intracortical connectivity.

neurons (Richardson et al., 2009), or adjustments of postsynaptic receptors. This refinement of thalamocortical connectivity however would have a limited impact on the tuning of total excitatory input, because the otherwise unselective intracortical connections would largely mask the effect of thalamocortical refinement (Fig. 5*C*, left).

Previously, a narrow critical time window (P11–P14) has been identified in the rat auditory cortex, during which the environmental sound frequencies the animal is exposed to can influence the cortical map of represented characteristic frequencies (de Villers-Sidani et al., 2007). Such cortical CF plasticity is believed to involve plasticity of thalamocortical connections (Buonomano and Merzenich, 1998; Hensch et al., 1998; Hensch, 2005; Khibnik et al., 2010), and it has been demonstrated that plasticity of thalamocortical synapses is lost after the critical period (Crair and Malenka, 1995; Isaac et al., 1997; Feldman et al., 1998; Jiang et al., 2007). It is interesting to note that during the developmental period we examined (P15–P25) which is much later than the critical period for cortical CF maps, the thalamocortical connections in A1 still undergo changes in the form of weight adjustments. On one hand, this result is consistent with the idea that the timing of critical periods is specific for different response features/properties examined (Insanally et al., 2009). On the other hand, it suggests that normal developmental maturation and critical-period-dependent cortical plasticity could be separate. More recently, there has been evidence that plasticity persists at mature thalamocortical synapses but is gated by presynaptic mechanisms (Blundon et al., 2011; Chun et al., 2013).

Our cortical silencing method effectively blocks firing of local A1 neurons, but would not affect long-range inputs such as callosal inputs and inputs from other cortical areas. This raises a possibility that the recorded thalamocortical response after cortical silencing may be contaminated by those long-range inputs. Although our data cannot exclude this possibility, we think that the contribution by those long-range cortical inputs is at most minimum because their projections do not or only sparsely terminate in L4 (Zhang et al., 2014; Rock and Apicella, 2015; Ibrahim et al., 2016).

Refinement of intracortical circuits plays a more critical role

During the period of refinement, the relative contribution of thalamocortical excitation to the total excitation at the optimal frequency decreased from ~60% to less than one-third. The latter value is consistent with what has been observed in other sensory systems or species at adult ages (Lien and Scanziani, 2013; L. Y. Li et al., 2013; Y. T. Li et al., 2013). Considering that the overall strength of thalamocortical excitation does not significantly decrease (Fig. 2*H*), our results suggest that the intracortical recurrent excitation is greatly strengthened. Moreover, the response ratio at non-optimal frequencies remained largely unchanged, indicating that the development of recurrent excitatory connectivity is marked by a selective strengthening of those inputs representing the same optimal frequency of the L4 neuron of interest. This can be achieved by strengthening the connections with nearby excitatory neurons, which have similar frequency selectivity as the target cell (Issa et al., 2014). Such frequency-specific strengthening of recurrent excitatory connections drives the sharpening of the tuning of intracortical excitation, which becomes even more selective than thalamocortical excitation (Fig. 5*C*, right). Even without increasing the selectivity of thalamocortical connectivity, sharpening of intracortical connectivity alone can qualitatively recapitulate the experimental observation (Fig. 5*D*). Therefore, our experimental data and modeling results both highlight a more critical role of developmental reorganization at the intracortical circuit level during this period of refinement.

Potential mechanisms underlying maturation of intracortical circuits

What could be the mechanisms underlying the revealed development of intracortical connections? In the visual cortex, it has been reported that during the postnatal development after eye opening, more recurrent excitatory connections are formed preferentially between neurons with similar functional responses, whereas connections between visually unresponsive neurons are lost (Ko et al., 2013). Dark rearing partially affects the formation of selective recurrent connections between neurons with similar functional responses and largely prevents the loss of connections between nonresponsive neurons (Ko et al., 2014). In the barrel cortex, it is found that sensory experience drives a threefold increase of local excitatory connectivity in L4 during postnatal development, resulting in a highly recurrent cortical network (Ashby and Isaac, 2011). In the auditory cortex, noise rearing during a critical period disrupts the functional maturation of tonal receptive fields, resulting in broad and unselective frequency tuning of cortical neurons (Sanes and Constantine-Paton, 1985; Zhang et al., 2002; Chang and Merzenich, 2003; de Villers-Sidani et al., 2007).

Based on those previous results, we propose that the selective strengthening of intracortical excitatory connections is driven by normal auditory experience during an early postnatal developmental period. It will be of great interest to examine in the future whether noisy rearing environments disrupt the normal developmental sharpening of excitatory input to L4 neurons at both thalamocortical and intracortical levels.

References

Antolík J, Hofer SB, Bednar JA, Mrsic-Flogel TD (2016) Model constrained by visual hierarchy improves prediction of neural responses to natural scenes. PLoS Comput Biol 12:e1004927. CrossRef Medline

Ashby MC, Isaac JT (2011) Maturation of a recurrent excitatory neocortical circuit by experience-dependent unsilencing of newly formed dendritic spines. Neuron 70:510–521. CrossRef Medline

Barkat TR, Polley DB, Hensch TK (2011) A critical period for auditory thalamocortical connectivity. Nat Neurosci 14:1189–1194. CrossRef Medline

Blundon JA, Bayazitov IT, Zakharenko SS (2011) Presynaptic gating of postsynaptically expressed plasticity at mature thalamocortical synapses. J Neurosci 31:16012–16025. CrossRef Medline

Bonham BH, Cheung SW, Godey B, Schreiner CE (2004) Spatial organization of frequency response areas and rate/level functions in the developing AI. J Neurophysiol 91:841–854. CrossRef Medline

Buonomano DV, Merzenich MM (1998) Cortical plasticity: from synapses to maps. Annu Rev Neurosci 21:149–186. CrossRef Medline

Chang EF, Merzenich MM (2003) Environmental noise retards auditory cortical development. Science 300:498–502. CrossRef Medline

Chang EF, Bao S, Imaizumi K, Schreiner CE, Merzenich MM (2005) Development of spectral and temporal response selectivity in the auditory cortex. Proc Natl Acad Sci U S A 102:16460–16465. CrossRef Medline

Chun S, Bayazitov IT, Blundon JA, Zakharenko SS (2013) Thalamocortical long-term potentiation becomes gated after the early critical period in the auditory cortex. J Neurosci 33:7345–7357. CrossRef Medline

Crair MC, Malenka RC (1995) A critical period for long-term potentiation at thalamocortical synapses. Nature 375:325–328. CrossRef Medline

de Villers-Sidani E, Chang EF, Bao S, Merzenich MM (2007) Critical period window for spectral tuning defined in the primary auditory cortex (A1) in the rat. J Neurosci 27:180–189. CrossRef Medline

Dorrn AL, Yuan K, Barker AJ, Schreiner CE, Froemke RC (2010) Developmental sensory experience balances cortical excitation and inhibition. Nature 465:932–936. CrossRef Medline

Eggermont JJ (1991) Maturational aspects of periodicity coding in cat primary auditory cortex. Hear Res 57:45–56. CrossRef Medline

Ehret G (1983) Development of hearing and response behavior to sound stimuli: behavioral studies. In: Development of auditory and vestibular systems (Romand R ed), pp 211–237. New York: Academic.

Etxeberria A, Hokanson KC, Dao DQ, Mayoral SR, Mei F, Redmond SA, Ullian EM, Chan JR (2016) Dynamic modulation of myelination in response to visual stimuli alters optic nerve conduction velocity. J Neurosci 36:6937–6948. CrossRef Medline

Fagiolini M, Pizzorusso T, Berardi N, Domenici L, Maffei L (1994) Functional postnatal development of the rat primary visual cortex and the role of visual experience: dark rearing and monocular deprivation. Vision Res 34:709–720. CrossRef Medline

Feldman DE, Nicoll RA, Malenka RC, Isaac JT (1998) Long-term depression at thalamocortical synapses in developing rat somatosensory cortex. Neuron 21:347–357. CrossRef Medline

Hackett TA, Barkat TR, O'Brien BM, Hensch TK, Polley DB (2011) Linking topography to tonotopy in the mouse auditory thalamocortical circuit. J Neurosci 31:2983–2995. CrossRef Medline

Hensch TK (2005) Critical period plasticity in local cortical circuits. Nat Rev Neurosci 6:877–888. CrossRef Medline

Hensch TK, Gordon JA, Brandon EP, McKnight GS, Idzerda RL, Stryker MP (1998) Comparison of plasticity *in vivo* and *in vitro* in the developing visual cortex of normal and protein kinase A RIβ-deficient mice. J Neurosci 18:2108–2117. CrossRef Medline

Ibrahim LA, Mesik L, Ji XY, Fang Q, Li HF, Li YT, Zingg B, Zhang LI, Tao HW (2016) Cross-modality sharpening of visual cortical processing through layer-1-mediated inhibition and disinhibition. Neuron 89:1031–1045. CrossRef Medline

Inan M, Crair MC (2007) Development of cortical maps: perspectives from the barrel cortex. Neuroscientist 13:49–61. CrossRef Medline

Insanally MN, Köver H, Kim H, Bao S (2009) Feature-dependent sensitive periods in the development of complex sound representation. J Neurosci 29:5456–5462. CrossRef Medline

Isaac JT, Crair MC, Nicoll RA, Malenka RC (1997) Silent synapses during development of thalamocortical inputs. Neuron 18:269–280. CrossRef Medline

Issa JB, Haeffele BD, Agarwal A, Bergles DE, Young ED, Yue DT (2014) Multiscale optical Ca^{2+} imaging of tonal organization in mouse auditory cortex. Neuron 83:944–959. CrossRef Medline

Jiang B, Treviño M, Kirkwood A (2007) Sequential development of long-term potentiation and depression in different layers of the mouse visual cortex. J Neurosci 27:9648–9652. CrossRef Medline

Katz LC, Shatz CJ (1996) Synaptic activity and the construction of cortical circuits. Science 274:1133–1138. CrossRef Medline

Khibnik LA, Cho KK, Bear MF (2010) Relative contribution of feedforward excitatory connections to expression of ocular dominance plasticity in layer 4 of visual cortex. Neuron 66:493–500. CrossRef Medline

Kim H, Gibboni R, Kirkhart C, Bao S (2013) Impaired critical period plasticity in primary auditory cortex of fragile X model mice. J Neurosci 33:15686–15692. CrossRef Medline

Ko H, Cossell L, Baragli C, Antolik J, Clopath C, Hofer SB, Mrsic-Flogel TD (2013) The emergence of functional microcircuits in visual cortex. Nature 496:96–100. CrossRef Medline

Ko H, Mrsic-Flogel TD, Hofer SB (2014) Emergence of feature-specific connectivity in cortical microcircuits in the absence of visual experience. J Neurosci 34:9812–9816. CrossRef Medline

Li LY, Li YT, Zhou M, Tao HW, Zhang LI (2013) Intracortical multiplication of thalamocortical signals in mouse auditory cortex. Nat Neurosci 16:1179–1181. CrossRef Medline

Li YT, Ibrahim LA, Liu BH, Zhang LI, Tao HW (2013) Linear transformation of thalamocortical input by intracortical excitation. Nat Neurosci 16:1324–1330. CrossRef Medline

Liang F, Li H, Chou X, Zhou M, Zhang NK, Xiao Z, Zhang KK, Tao HW, Zhang LI (2018) Sparse representation in awake auditory cortex: cell-type dependence, synaptic mechanisms, developmental emergence, and modulation. Cereb Cortex. Advance online publication. Retrieved October 11, 2018. doi: 10.1093/cercor/bhy260

Lien AD, Scanziani M (2013) Tuned thalamic excitation is amplified by visual cortical circuits. Nat Neurosci 16:1315–1323. CrossRef Medline

Liu BH, Wu GK, Arbuckle R, Tao HW, Zhang LI (2007) Defining cortical frequency tuning with recurrent excitatory circuitry. Nat Neurosci 10:1594–1600. CrossRef Medline

Liu BH, Li P, Sun YJ, Li YT, Zhang LI, Tao HW (2010) Intervening inhibition underlies simple-cell receptive field structure in visual cortex. Nat Neurosci 13:89–96. CrossRef Medline

Metherate R, Aramakis VB (1999) Intrinsic electrophysiology of neurons in thalamorecipient layers of developing rat auditory cortex. Brain Res Dev Brain Res 115:131–144. CrossRef Medline

Mrsic-Flogel TD, Schnupp JW, King AJ (2003) Acoustic factors govern developmental sharpening of spatial tuning in the auditory cortex. Nat Neurosci 6:981–988. CrossRef Medline

Polley DB, Thompson JH, Guo W (2013) Brief hearing loss disrupts binaural integration during two early critical periods of auditory cortex development. Nat Commun 4:2547. CrossRef Medline

Read HL, Winer JA, Schreiner CE (2002) Functional architecture of auditory cortex. Curr Opin Neurobiol 12:433–440. CrossRef Medline

Richardson RJ, Blundon JA, Bayazitov IT, Zakharenko SS (2009) Connectivity patterns revealed by mapping of active inputs on dendrites of thalamorecipient neurons in the auditory cortex. J Neurosci 29:6406–6417. CrossRef Medline

Rock C, Apicella AJ (2015) Callosal projections drive neuronal-specific responses in the mouse auditory cortex. J Neurosci 35:6703–6713. CrossRef Medline

Romand R (1997) Modification of tonotopic representation in the auditory system during development. Prog Neurobiol 51:1–17. CrossRef Medline

Salami M, Itami C, Tsumoto T, Kimura F (2003) Change of conduction velocity by regional myelination yields constant latency irrespective of distance between thalamus and cortex. Proc Natl Acad Sci U S A 100:6174–6179. CrossRef Medline

Sanes DH, Constantine-Paton M (1985) The sharpening of frequency tuning curves requires patterned activity during development in the mouse, *Mus musculus*. J Neurosci 5:1152–1166. CrossRef Medline

Seybold BA, Phillips EAK, Schreiner CE, Hasenstaub AR (2015) Inhibitory actions unified by network integration. Neuron 87:1181–1192. CrossRef Medline

Sun YJ, Wu GK, Liu BH, Li P, Zhou M, Xiao Z, Tao HW, Zhang LI (2010) Fine-tuning of pre-balanced excitation and inhibition during auditory cortical development. Nature 465:927–931. CrossRef Medline

Sun YJ, Kim YJ, Ibrahim LA, Tao HW, Zhang LI (2013) Synaptic mechanisms underlying functional dichotomy between intrinsic-bursting and regular-spiking neurons in auditory cortical layer 5. J Neurosci 33:5326–5339. CrossRef Medline

Tan AY, Zhang LI, Merzenich MM, Schreiner CE (2004) Tone-evoked excitatory and inhibitory synaptic conductances of primary auditory cortex neurons. J Neurophysiol 92:630–643. CrossRef Medline

Winer JA, Miller LM, Lee CC, Schreiner CE (2005) Auditory thalamocortical transformation: structure and function. Trends Neurosci 28:255–263. CrossRef Medline

Wu GK, Arbuckle R, Liu BH, Tao HW, Zhang LI (2008) Lateral sharpening of cortical frequency tuning by approximately balanced inhibition. Neuron 58:132–143. CrossRef Medline

Zhang LI, Bao S, Merzenich MM (2001) Persistent and specific influences of early acoustic environments on primary auditory cortex. Nat Neurosci 4:1123–1130. CrossRef Medline

Zhang LI, Bao S, Merzenich MM (2002) Disruption of primary auditory cortex by synchronous auditory inputs during a critical period. Proc Natl Acad Sci U S A 99:2309–2314. CrossRef Medline

Zhang S, Xu M, Kamigaki T, Hoang Do JP, Chang WC, Jenvay S, Miyamichi K, Luo L, Dan Y (2014) Selective attention. long-range and local circuits for top-down modulation of visual cortex processing. Science 345:660–665. CrossRef Medline

Zhou Y, Liu BH, Wu GK, Kim YJ, Xiao Z, Tao HW, Zhang LI (2010) Preceding inhibition silences layer 6 neurons in auditory cortex. Neuron 65:706–717. CrossRef Medline